Title
Performance, prediction, optimization, and user behavior of night ventilation

Journal
Energy and Buildings, 166

ISSN
03787788

Authors
Landsman, Jared
Brager, Gail
Doctor-Pingel, Mona

Publication Date
2018-05-01

DOI
10.1016/j.enbuild.2018.01.026

Peer reviewed

Performance, Prediction, Optimization, and User Behavior of Night Ventilation

Jared Landsman[a1], Gail Brager[a], Mona Doctor-Pingel[b]

[a] *Department of Architecture, University of California, Berkeley, 230 Wurster Hall, Berkeley, CA, USA*
[b] *Auroville Center for Scientific Research, Auroville, India*

Abstract

Previous studies have demonstrated a potential reduction in cooling load and improvement in comfort from the implementation of night ventilation. This paper describes the performance, in terms of indoor environmental conditions, of three buildings from both the U.S. and India that use night ventilation as their primary cooling method. The research methods used the following approach: 1) Assess the cooling strategy in relation to the adaptive comfort model; 2) Develop a hybrid model, using both first principle equations and the collected data, to predict the instantaneous air and mass temperatures within each building and use the model to assess performance of the cooling strategy; 3) Determine an optimized ventilation control strategy for each building to minimize energy and maintain comfortable temperatures. 4) Develop a statistical model using collected data to predict the window opening pattern for occupants of a building using natural night ventilation. The study yielded the following results: 1) The buildings in the mild climate are successfully keeping the indoor temperature low, but also tend to be overcooling; 2) The night ventilation strategy has very little impact on indoor conditions of the buildings in the mild climate; 3) The impact of night ventilation is less significant when there is low internal loads and heavy mass; 4) The building in the hot and humid climate is keeping the indoor temperature within the comfort bounds for 88% of the year; 5) The night ventilation strategy has advantageous impact on indoor conditons of the building in the hot and humid climate, but not enough to cool the space on its own; 6) Model predictive control has the potential to further improve the performance of night ventilation. 7) Window opening behavior for the building using natural night ventilation is most heavily dependent on indoor air temperature and mass temperature.

Keywords: Night ventilation; Passive cooling; Model predictive control; User behavior

1. Introduction

1.1 Background

Many developing countries currently undergoing economic growth and urbanization are also experiencing increased energy consumption due to the following of western design practices, such as mechanical cooling. The prevalence of air conditioning in both the developed and developing world has also had the consequence of increased comfort expectations. As the developing world continues to urbanize and their energy regulations continue to get more stringent, it will become even more necessary to find low-energy solutions to cooling before the use of energy-intensive mechanical cooling becomes the norm all over the world. One passive design strategy that has been of interest to researchers for the last 30 years or so is night ventilation. Night ventilation is a passive or semi-passive cooling technique that utilizes the outdoor diurnal temperature swing and the building's thermal mass to pre-cool a building through increased outdoor airflow at night. At night, when the outdoor air temperature is lower than during the daytime, the increased airflow cools down the mass, allowing it to release the heat that was stored during the previous day. During the following day, the cooler mass serves as a heat sink to absorb

[1] Corresponding author. Tel.: 201 463 4568
Email address: jlandsman6192@gmail.com

 https://doi:10.1016/j.enbuild.2018.01.026
www.escholarship.org/uc/item/9jk1d795

the heat present in the space from solar and internal loads (Givoni 1992a; M. Santamouris et al. 1996; Artmann, Manz, and Heiselberg 2007).

There are three categories of night ventilation. The first is natural, or passive, night ventilation, which simply ventilates the spaces by naturally induced airflow through openings in the building's envelope, typically windows or air vents (Geros et al. 1999). The second category is mechanical night ventilation, which utilizes air ducts along with supply and exhaust fans to provide airflow in the space (Geros et al. 1999). During the day, air is supplied into the space at a code-required minimum airflow rate. Although this requires a small amount of energy for fan use, it is also a much more controlled and predictable system, and is usually completely automated so there is no manual daily control required from the occupants. The final category is hybrid ventilation, which can include the combined use of natural and mechanical ventilation at different times of the day or year in the same space, at the same time in different rooms, or at the same time in the same space. A hybrid night ventilation system allows for more flexibility in the control of the system and associated energy usage.

This work was guided by methods used by previous researchers, and a more complete literature review can be found in Landsman (2016). A brief summary follows.

Field study methods. Givoni (1998) looked at the performance of night ventilation by monitoring three buildings, each having an identical floor plan, but with different levels of thermal mass. Blondeau et al. (1997) studied the performance of night ventilation in a three-level office and classroom building, monitoring four rooms over a one-month period, three of which under night ventilation and one of which was not night ventilated, to be used as a reference room. Geros et al. (1999) looked at the performance of night ventilation in two air conditioned buildings and one free floating building, monitoring each for a period of one to three weeks under four different conditions of varying night ventilation usage and mechanical systems usage (free floating vs. thermostatically controlled). Pfafferott et al. (2003, 2004) did two studies, one looking at the relationship between night ventilation efficiency and air change rate, solar gains, and internal gains, and the other studies the efficiency of night ventilation in an office building in Germany. Finn et al. (2007) studied a night-ventilated library, looking at the impact of different design and operational parameters on the strategy's success over a period of four weeks. For two summer months, Kubota et al. (2009) looked at the performance of night ventilation in two unoccupied homes of identical size, design and construction.

Modelling methods. Occupant behavior is one of the most difficult components of a building to model because occupants do not always follow a specific pattern. However, numerous studies have been conducted to model occupant behavior, specifically with regard to window opening patterns. Yun and Steemers (2008, 2010) conducted two studies that examined the occupant window-usage for a naturally night ventilated building. These studies used a logistic regression model and a probit regression model, with variables including indoor air temperature, outdoor air temperature, time of day, and previous window state. Model predictive control (MPC) is an emerging topic in the field of building automation due to its enabling of effective control systems that can operate without expert intervention (García, Prett, and Morari, 1989). To successfully execute model predictive control, one must obtain data, develop a model to predict interior conditions, train the model and then implement that model in a control sequence. The key to model generation, but one that is difficult to achieve, is finding a model that is simple enough to minimize computation time but complex enough to minimize error. There are two approaches to developing a model for MPC. The first is black-box, meaning the model is based solely on historical data from building monitoring and does not reflect the physical properties of the building construction or systems (Vidrih, Arkar, and Medved 2016). The second method is white-box, meaning the model relies only on physical properties of the building and not on historical data. There are also hybrid models that combine features of both, such as the work of Zhang et al. (2014), which used simplified resistance/capacitance equations to represent the heat transfer between the thermal mass, indoor air, and exterior. After the model is validated, it can then be paired with weather forecasts to predict future conditions inside the building. Medved et al. (2014) used a TRNSYS simulation, along with weather forecasts for the following 24-h period, to predict the time-dependent night cooling potential and cooling load for the following day. The model can also be used to optimize the night ventilation strategy, helping determine when the building should enter and exit night ventilation mode. Zhang et al. (2014) optimized their model by minimizing the energy consumed by cooling coils and fans, while setting constraints of minimum airflow rate equal to the ASHRAE 62.1 acceptable indoor air quality limit, and supply temperature greater than 16 °C, to reduce local discomfort.

Parameter influence on night ventilation. Comfort improvement is strongly dependent on good control over heat gains from solar loads, equipment, occupants, and conduction through building fabric (Blondeau et al., 1997). Most studies suggest that lower internal loads allow for improved night ventilation performance. Kolokotroni et al. (1999a) conducted an experiment that showed increasing heat gains diminished the effectiveness of night ventilation. Geros et al. (1999) showed that night ventilation efficiency increased during an experimental period with lower convective and radiative internal gains. Artmann et al. (2008) ran a study in which overheating degree hours increased by a factor of 2-2.5 when heat gains from office equipment increased from 50 to 150 W per person. On the whole, it is believed that night ventilation improves as exposed thermal mass increases (Kolokotroni and Aronis, 1999). This has been seen during experiments in which night ventilation lowered the indoor maximum temperature more so in a high-mass building than in a low-mass building (Finn et al., 2007; Givoni, 1998; Shaviv et al., 2001). Interestingly, when thermal mass is present in the walls, the magnitude of its effect on night ventilation changes depending on the size of the room. As the room volume decreases and the ratio of wall to floor area decreases, the size of the thermal mas becomes less significant (Artmann et al., 2008). It is universally agreed upon that increased airflow corresponds to increased night ventilation performance. Experiments have shown that higher airflow rates lead to increased energy savings for all forms of natural ventilation and that an increase in air change rate increases the cooling effect of night ventilation (Kolokotroni and Aronis, 1999; Pfafferott et al., 2003). That being said, there is some disagreement on the returns of an incremental escalation in airflow rate. Some studies did not note any comfort improvement beyond 10 air changes per hour (Blondeau et al., 1997; Finn et al., 2007), while one study saw significant improvements in comfort up to 20 air changes per hour (Artmann et al., 2008). Some studies found that an increase from 10 to 30 air changes per hour led to an average decrease of peak indoor temperature from 1.8 °C to 2.2 °C (Geros et al. 1999). On the other hand, one study perceived a plateau of maximum indoor air temperature by the airflow rate of 20 air changes per hour (Shaviv, Yezioro, and Capeluto 2001).

The most significant control parameters of all mechanical night ventilation systems are setpoint temperature and hours of night ventilation operation. One study found that an increase of setpoint temperature from 24 °C to 27 °C led to an increase of energy savings due to night ventilation from 5% to 8%, and that five extra hours of night ventilation operation increased energy savings from 5% to 7% (Kolokotroni and Aronis, 1999). Another study saw a reduction in overheating hours due to night ventilation of 39-51% at a setpoint temperature of 25 °C, 69-79% at a setpoint temperature of 27 °C, and 92-96% at a setpoint temperature of 29 °C (Geros et al., 1999). Interestingly, one experiment has shown increased energy usage from no night ventilation to mechanical night ventilation in a medium weight office building, due to the increased operation of fans (Kolokotroni and Aronis 1999a).

The most crucial parameters are those related to climate. Experiments have shown that a reduction of outdoor night-time temperature corresponds with an increase in night ventilation system capacity and lower internal morning temperatures (Artmann et al., 2008; Kolokotroni et al., 1998; Pfafferott et al., 2003; Santamouris and Asimakopoulos, 1996). Research has shown that this relationship between internal temperature and outdoor temperature in warm climates is stronger when the outdoor temperature is high and weaker when outdoor temperature is low, suggesting that user behavior and internal loads have a stronger effect on internal temperature at lower outdoor temperatures (Pfafferott et al., 2004). It has also been seen that lower outdoor temperature amplitude, or diurnal swing, leads to a lower cooling potential for night ventilation (Geros et al., 1999).

1.2 Research objective

The first objective of this study is to understand the control strategy and performance expectations of three real buildings using different night ventilation control strategies (automated mechanical, automated natural, and manual natural) coupled with thermal mass. The second objective is to make generalizable statements about the performance of night ventilation that can help engineers and architects effectively design for the strategy, specifically with regard to climate, program, level of mass, and type of ventilation system. This is done by assessing the measured performance of each building with respect to the adaptive comfort model, and then by assessing the effect of the strategy on indoor conditions using both measured data and a temperature prediction model. The third objective is to optimize the ventilation control strategy for each building to minimize the amount of time outside of the comfort bounds.

2. Building and climate descriptions

Following the building selection approach taken by Geros et al. (1999), our methodology looked into three different buildings each with different levels of thermal mass and night ventilation strategies, both free floating and thermostatically controlled facilities. The first case study, La Escuelita Elementary School (LEES), is an elementary school that is part of the Oakland Unified School District (see details in Table 1 for many of the parameters described below). The school is located in Oakland, CA, which has a fairly mild climate and low humidity. The temperature ranges from about -1-32 °C (30-90 °F) throughout the year, with only 20 days going above 27 °C (80 °F). The average diurnal swing is 8 °C (15 °F), sometimes going as high as 20 °C (36 °F).

Each classroom contains thermal mass in the form of a 4-inch concrete slab (145 pcf) and 2-inch cement plaster walls (95 pcf). The floor and walls both have embedded temperature sensors and varying depths. Of the classrooms studied here, two are located on the ground floor and six are located on the second floor, each with varying area and position. The facility uses fan-assisted mechanical ventilation for cooling, and the controls were designed by Taylor Engineering. During occupied hours (8am – 4pm), the variable air volume (VAV) box for each classroom will supply the room with the minimum amount of airflow to meet the code requirements, V_{min}, through displacement ventilation. The displacement diffusers provide 100% outdoor air from central air handling units. When windows are opened in a space, a switch disables the HVAC system. If the outdoor air temperature is low, the room is ventilated by displacement ventilation, which creates a temperature stratification in the space. If the indoor air temperature exceeds the cooling setpoint (23.3 °C (74 °F) in perimeter rooms, 22.8 °C (73 °F) in interior rooms), the system relies on increased airflow to cool its occupants. When the space overheats, the airflow rate will ramp up to the occupied cooling airflow setpoint, $V_{cool,occ}$ (see Table 1 for values) and ceiling fans are activated. The mechanical system is designed to enter night ventilation mode, which consists of ramping up the airflow to the unoccupied cooling airflow setpoint, $V_{cool,unocc}$, when the following conditions are met:

1. The classroom is unoccupied
2. The classroom is within 8 hours of the expected start of occupancy the following day
3. The floor surface temperature is at least 0.56 °C (1 °F) higher than the mass temperature setpoint
4. The outdoor air temperature is at least 5.6 °C (10 °F) below the floor temperature

As per design, the mass temperature setpoint is set equal to the heating setpoint of 21.1 °C (70 °F) in order to avoid unnecessary warmup after night ventilation. Mass temperature was chosen as a setpoint because it was assumed that the indoor air temperature would not reflect the necessity of night ventilation due to the fact that the air temperature was so dependent on occupancy loads. The system will leave night ventilation mode when the floor temperature falls below the mass temperature setpoint. Mechanical night ventilation was chosen over natural night ventilation to ensure better security of the building and control over the indoor conditions. The system will sometimes enter a "warm-up mode" the morning after night ventilation if the indoor air temperature is below the heating setpoint.

Classroom	Story	Position	Area (ft^2)	V_{min} (CFM)	$V_{cool,occ}$ (CFM)	$V_{cool,unocc}$ (CFM)
110	1st	N	1240	215	1800	1800
120	1st	NE	1185	230	1900	1900
233	2nd	NW	930	175	1500	1500
234	2nd	NW	930	140	1100	1100
235	2nd	W	960	145	1200	1200
240	2nd	S	1050	140	1100	1100
241	2nd	SE	1020	140	1100	1100
242	2nd	SE	1020	185	1500	1500

Table 1. LEES classroom physical and system parameters

The second case study is 435 Indio Way (IND), an open-plan office located in Sunnyvale, CA, which also has a mild climate and low humidity. The temperature ranges from about -1-37.8 °C (30-100 °F) throughout the year, with only 44 days going above 27 °C (80 °F). The average diurnal swing is 9.4 °C (17 °F), sometimes going as high as 17.8 °C (32 °F).

The facility, which was recently renovated to become net zero energy, is approximately 3,000 m^2 (32,000 ft^2). The structure of the building is comprised of 12-inch thick concrete walls and exposed concrete slab, both of which are left over from the existing building structure. IND also makes use of electrochromic windows to block solar radiation, in addition to solar PV panels as a renewable source of energy. IND uses automated natural night ventilation to pre-cool the building. During occupied hours (6am-8pm), the space is almost never cooled mechanically. The system enters night ventilation mode by opening up the windows and skylights under the following conditions:

1. The space is unoccupied
2. The indoor air temperature is greater than 21.1 °C (70 °F)
3. The outdoor air temperature is less than 20 °C (68 °F)

Unlike LEES, mass temperature is not one of the criteria for the operating algorithm. The systems leaves night ventilation mode when the indoor air temperature falls below 20.6 °C (69 °F). Air temperature was chosen as a threshold rather than mass temperature because there were no embedded mass temperature sensors in the original design. The setpoints were chosen as the lowest temperatures needed to keep the next day's indoor temperature below the upper comfort limit in the design team's model. The setpoints were then optimized by the building operator through trial and error.

The third case study is called the Blessing House (BH), a two-story residential building located in Auroville, India, which has a hot and humid climate, with an average relative humidity of 60%. The temperature ranges from about 16-40 °C (60.8-104 °F) throughout the year, almost all of which go above 28 °C (82.4 °F). Auroville sees an average diurnal swing of about 9 °C (16.2 °F), sometimes going as high as 15 °C (27 °F). The Pre-Monsoon and Monsoon seasons tend to have higher temperatures (averaging 30 °C (86 °F)) and higher diurnal swing (averaging 10 °C (18 °F)) than Post-Monsoon and Winter seasons. Humidity levels in the house are high, ranging from 70 to 95%, due to the local humid climate but even increased by the surrounding (forest environment).

BH has thermal mass in its floor, roof, and walls. The building's walls consist of a composite wall assembly - compressed earth blocks (290x140x90 mm) on the internal side, Aerocon blocks (600x200x75 mm) on the external side and a layer of cement plaster (20 mm thick) on both sides. The building's ceiling/roof construction is an insulated assembly and consists of white reflective ceramic tiles, Aerocon blocks (300x300x50 mm), a layer of 5 cm cement concrete, followed by Hurdi terra cotta hollow blocks with reinforcement, and a layer of cement plaster (20 mm thick). The building is fully solar powered with invertor and battery back up. The rainwater is collected into a pool which is used thoughout the year for swimming by the occupants and used for watering the garden around. A solar water heater provides for hot water. Most windows (except in a small bedroom area) are single glazed float glass with aluminium frame. Full house is grilled with metal sections with wriemesh to make it mosquito proof. The space of interest to this case study is a room on the second floor, 24 m^2 in area, with a ceiling slanting from 3 m to 4.6 m. It has a overhang of 1.2 mt (4 ft) on the northern side.

This facility uses occupant controlled natural night ventilation to pre-cool the house. This means the occupants manually open their windows at night and close them in the morning at their own discretion. The windows are closed in the morning at a yearly average time of approximate 9:00AM. For the three seasons (summer, winter, monsoon), there was a clear pattern of closing the window between 7:30-830am, which could be due to a working schedule starting between 8:30 – 9:00 AM. The windows are opened the night at a yearly average time of 19:10pm. The opening times are more spread out than for the closing, and typically occues more than one hour later in the winter compared to both the other seasons. This span in the opening hour could be explained by a more adaptable schedule of the occupant in the evening, since after-work and night activities can change the time of return of the occupants.

3. Methodology

A thorough description of the methods is beyond the space limitations of this paper, and details such as sensor accuracy, data intervals, comfort standard acceptability limit calculations, and optimization equations can be found in Landsman (2016).

3.1 Data collection

The parameters measured at each location is summarized in Table 2. Indoor conditions from LEES were collected through the building management system (BMS), which retrieved temperature data from PreCon Encapsulated Thermistor Sensors. Data was available for all eight classrooms being studied for the dates of July 2nd, 2015 to Oct 6th 2015. Indoor conditions from IND were also collected through the BMS, using Veris CW sensors. Data was available for the open-plan office for the dates of Sept 1st, 2015 to Oct 31st, 2015 (see table 2). In addition, daily energy loads were obtained for one year, broken down by submeter, and hourly loads were estimated based on this data. For both LEES and IND, hourly outdoor air temperature was obtained from the National Oceanic and Atmospheric Association's Climatic data center, for the closest weather station to the buildings.

Data collection for BH was carried out following the methodology laid out by Finn et al. (2007), collecting indoor air temperature and internal wall surface temperature through HOBO U12 data loggers. As done by Pfafferott et al. (2004), short-term data collection was done using an Extech HT 30 globe temperature meter to cross-check the long term measurements. The data was collected for the dates of Oct 22nd, 2013 to Oct 14th, 2014 in hourly time intervals. Using the procedure taken by Gagliano et al. (2014), hourly outdoor air temperature and solar radiation were pulled from the Auroville weather station. While air movement is certainly important for thermal comfort in hot and humid climates, this data was not collected in BH due to limitations in available sensors (the kinds of sensors required for continuous and accurate measurements of the typically low velocities found indoors are quite expensive). Such data would be important to gather, however, for field studies of daytime comfort, but this was the beyond the scope of this study.

Parameter	LEES	IND	BH
Outdoor air temperature	X	X	X
Indoor air temperature	X	X	X
Mass wall temperature	X	X	X
Mass floor temperature	X		
Supply temperature	X		
Airflow rate	X		
Window state		X	X
Relative humidity			X
Internal load		X	
Solar radiation			X

Table 2. Collected data from each case study

3.2 Temperature model generation

In order to implement model predictive control, models needed to be generated for each building/room to capture the physical and thermal characteristics of the building construction and HVAC system. Following the approach taken by Zhang et al. (2014), hybrid (part black-box and part white-box) models were generated in Matlab by using collected data along with simplified resistance/capacitance dynamical equations. Once the first principles equations were established, model parameters were identified using the non-linear least squares method. Different model variations were tested using the k-fold cross validation technique. Finally, each model was validated against real building data. The nomenclature used in the model equations that follow is summarized in Table 3.

t	Time step [hr]
T	Temperature [°F or °C]
R	Thermal resistance [°F-hr/BTU or °C-hr/J]
C	Thermal capacitance [BTU/°F or J/°C]
V	Ventilation rate [ft^3/hr or m^3/sec]
s	Window or ventilation state [0/1]
r	Solar radiation [BTU or J]
int	Internal load [BTU or J]
ρ	Density [lb/ft^3 or kg/m^3]
c	Specific heat [BTU/lb-°F or J/kg-°C]
P	Power [BTU J]
N	# of data points
Subscript	
I	Indoor air
O	Outdoor air
W	Wall
F	Floor
V	Supply

Table 3. Model nomenclature

Numerous variations of dynamical equations were formulated to model the heat transfer for each case study. The dynamical equations for each building use some combination of the following:

1. Uncontrollable inputs of outdoor air temperature, solar radiation, and internal loads
2. Controllable inputs of supply temperature and airflow rate or window state
3. Outputs (or state variables) of indoor air temperature and mass temperature

The basic form of the dynamical equations takes the material capacitance multiplied by the time derivative of that material's temperature, and sets it equal to the sum of the temperature difference of each material divided by their respective resistance (see equation 2). Material capacitance and resistance encapsulates the physical properties in a simplified manner via single parameter values.

As done by Pfafferott et al. (2004), model parameters, such as thermal properties of walls and windows, were identified using a portion of collected data and a sensitivity analysis. The first step of parameter identification is choosing a portion of the data set as the training data for the model (see Landsman (2016) for the dates of the portions used from each dataset for this purpose). The next step is to calculate the persistence of excitation (PE). If all PE values are above zero, this indicates that the parameters are identifiable. The strategy used for identifying parameters is the nonlinear least squares method, as used by Moura et al. (2014), which minimizes the square error between the simulation results and the training data using equations 2 and 3, in which P is defined by equation 1, and J is a cost criteria to be minimized. Initial conditions for $\hat{\theta}$ were chosen based on approximated real thermal and physical properties of each building. The function then does 100 iterations for each parameter. Once a full set of iterations is complete, the initial conditions for $\hat{\theta}$ are replaced with the final values from the previous iteration of the nonlinear least squares function. This process is done anywhere from one to ten times, depending on how many iterations are needed until the simulation produces no further improvements in reducing the error. The nonlinear least squares method is performed in Matlab.

$$P(t) = \left[\int_{t_1}^{t_N} \phi(t)\phi^T(t)dt\right]^{-1} \quad (1)$$

$$J(\hat{\theta}) = \frac{1}{2}\int_{t_1}^{t_N}[z(t) - \hat{z}(t)]^2 dt \quad (2)$$

$$\frac{d\hat{\theta}(t)}{dt} = \mathrm{P}\epsilon\phi,\ \hat{\theta}(0) = \hat{\theta}_0,\ \frac{dP(t)}{dt} = -\mathrm{P(t)}\phi(t)\phi^T(t)P(t),\ P(0) = P_0 \quad (3)$$

Once parameters were identified, the model had to be simulated in order to calculate the model error. The dynamical equations were rearranged into a system of linear state-space equations (Eqn. 4), where A is a matrix of state variable parameters, B is a matrix of input variable parameters, x is a vector of state variables, and u is a vector of input variables. The state-space equations were then solved using initiation conditions chosen from the actual data set. This process was completed in Matlab.

$$\dot{x} = Ax + Bu,\ x(0) = x_0 \quad (4)$$

Once the model was simulated, different types of error parameters were calculated to determine the accuracy and precision of the models. Error metrics for this study were selected based on the literature review. The error metrics chosen for this analysis, including mean absolute error (MAE), standard deviation of absolute error (SDAE), mean absolute percent error (MAPE), standard deviation of absolute percent error (SDAPE), root mean square error (RMSE), and the coefficient of variation of the root mean square error (CVRMSE), were calculated using equations 5 through 8. In previous studies modeling night ventilation, the following have been considered acceptable errors for temperature data: 0.3 °C MAE, 0.46 °C mean bias deviation with 0.88 °C RMSE, and 1.14 °C mean bias deviation with 1.35 °C RMSE (Blondeau et al., 1997; Finn et al., 2007; Geros et al., 1999).

$$MAE = \frac{1}{N}\sum_{i=1}^{N}|z_i - \hat{z}_i|\ ,\ SDAE = \sqrt{\frac{1}{N}\sum_{i=1}^{N}(|z_i - \hat{z}_i| - MAE)^2} \quad (5)$$

$$MAPE = \frac{1}{N}\sum_{i=1}^{N}\frac{|z_i - \hat{z}_i|}{z_i},\ SDAPE = \sqrt{\frac{1}{N}\sum_{i=1}^{N}\left(\frac{|z_i - \hat{z}_i|}{z_i} - MAE\right)^2} \quad (6)$$

$$RMSE = \sqrt{\frac{1}{N}\sum_{i=1}^{N}|z_i - \hat{z}_i|^2} \quad (7)$$

$$CVRMSE = \frac{RMSE}{\frac{1}{N}\sum_{i=1}^{N} z_i} \quad (8)$$

Although the validation data set is not to be used during model generation in order to avoid overfitting, a method known as K-fold cross validation can be executed using only the training data set, as done by Tsanas, Athanasios, and Angeliki Xifara (2012). This method first divides the training data set into K equal portions (this study used ten). Next, parameters are identified using nonlinear least squares method, but only using one tenth of the original training data. Finally, the model is simulated with the other nine tenths of the training data, which are now being used as validation data, and the model errors are calculated. This process is iterated with each tenth of the data set being used as training data and the other nine tenths being used as validation data. K-fold cross validation can give information about how a model will run with data that was not used for parameter identification prior to the actual model validation. When the final model variations were selected, each model was validated using real measured data (again, see Landsman (2016) for the dates that were used from each dataset for this purpose).

3.3 Occupant behaviour model generation

To understand occupant behavior regarding the opening and closing of windows in Blessing House, a prediction model was generated based on environmental , indoor, and temporal parameters. This prediction model was established using the methodology of Yun and Steemers (2008, 2010). The objective of this model was to determine, based on specific parameters, whether the occupants will have the windows open or closed. To generate the model, specific variables were first selected as potential inputs, including outdoor variables (air temperature, relative humidity and wind velocity), indoor variables (air temperature, humidity, and mass temperature), and temporal inputs (season and hour). A subset of measured data for training the model was then chosen to match the training data for the temperature prediction model (see Landsman (2016) for specific dates). This data was subsequently used to form a regression, in which probit analysis was selected as the primary regression method. The probability of a window being open, P, is depicted in equation 9, in which each x-value is a different parameter and each α is a regression constant.

$$P = \frac{e^{\alpha_0+\alpha_1 x_1+\alpha_2 x_2+\dots}}{1+e^{\alpha_0+\alpha_1 x_1+\alpha_2 x_2+\dots}} \tag{9}$$

Once the probability is calculated for each timestep, it is then rounded up to 100% (indicating the window is open) or down to 0% (window is closed), and these predicted values can then be compared to measured window state. The error metric used to assess the accuracy of the model is simply the percentage of data for which the predicted window state matches the actual window state. Model variations with different input parameters were tested using the k-fold cross validation technique, and the final selected model variation was validated using a data set with dates that matched that for the temperature prediction model.

3.4 Baseline data analysis

Using the measured data from each building, analysis assessed the performance of night ventilation with regard to comfort and energy. First, trends of indoor air temperature, mass temperature, and instantaneous damping (Eqn. 10), the instantaneous difference between indoor and outdoor air temperature, were ascertained to determine if any daily or seasonal trends exist. Landsman (2016) provides details about how the "seasons" were defined for each location. Next, eight different comfort and energy metrics were calculated for individual days, described below and in the equations that follow:

1. Daily indoor maximum air temperature ($T_{I,max}$), the highest indoor air temperature occurring in a single day, as used by Givoni (1998).
2. Daily maximum damping (Eqn. 11), the difference between the peak indoor and peak outdoor daily air temperature.
3. Daily indoor temperature range (Eqn. 12), the difference between the highest and lowest indoor air temperature in a specific day.
4. Decrement factor (Eqn. 13), the daily indoor air temperature range over the daily outdoor air temperature range.
5. Daily time lag (Eqn. 14), the amount of time between peak outdoor air temperature and peak indoor air temperature, as used by Gagliano et al., 2014.
6. Daily energy removed (Eqn. 15a), the amount of heat removed from the space by airflow, also used by Blondeau et al. (1997), Medved et al. (2014), and Pfafferott et al. (2003).
7. Area normalized daily energy removed (Eqn. 15b), the daily energy removed normalized by the room area.
8. Potential energy efficiency (Eqn. 16), the daily energy removed normalized by the energy consumed by the fan.

Fan energy was estimated based on the fan motor power curve provided in the product specifications, while the COP was estimated as 4, based on the average COP for "best practice" heat pumps. Each of these metrics was then assessed across time.

$$Damp_{inst} = T_O - T_I \tag{10}$$
$$Damp_{max} = T_{O,max} - T_{I,max} \tag{11}$$
$$T_{I,range} = T_{O,max} - T_{I,min} \tag{12}$$
$$f = \frac{T_{I,max}-T_{I,min}}{T_{O,max}-T_{O,min}} \tag{13}$$

$$\varphi = t(T_{O,max}) - t(T_{I,max}) \tag{14}$$

$$Q = \int_{t_1}^{t_N} V\,\rho_{air} c_{air}\big(T_I(t) - T_O(t)\big)dt,\ \ Q_{norm} = \frac{\int_{t_1}^{t_N} V\,\rho_{air} c_{air}\big(T_I(t) - T_O(t)\big)dt}{Area} \tag{15}$$

$$PEE = \left(\frac{Q}{COP}\right)/Q_{fan} \tag{16}$$

3.5 Comparison to comfort standards

Each data set was then compared to the Adaptive Comfort Standard (ACS) for naturally ventilated buildings in ASHRAE Std 55 (2013). This standard is based on experiments conducted all over the world, including tropical regions, and is a function of running mean outdoor air temperature (de Dear and Brager 1998). For the purposes of this analysis, a homogenous mean radiant temperature was estimated based on the area weighted surface temperature (Eqn. 17). BH data was additionally compared to the newly created India Model for Adaptive Comfort (IMAC) (Manu et al. 2016). For these comparisons, discomfort degree hours (DDH), as used by Pfafferott et al. (2003, 2004) and Artmann et al. (2008) were calculated for each case (Eqns. 18A, 18B). DDH is the sum of the difference between the indoor temperature and a specified temperature threshold across all time steps, multiplied by a given number of time steps. This is most commonly done across one day or one year. For the critical temperature for the DDH calculation, the ACS or IMAC upper and lower 80% acceptability limit were used for occupied hours.

$$T_{mr} = \frac{\sum T_{S,i} A_i}{\sum A_i} \tag{17}$$

$$DDH_{+} = \sum_{t=1}^{N} h_t (T_{op,t} - T_{crit,t}) \begin{cases} h_t = 1\ h \text{ if } T_{op,t} \geq T_{crit,t} \\ h_t = 0 \quad \text{if } T_{op,t} < T_{crit,t} \end{cases} \tag{18A}$$

$$DDH_{-} = \sum_{t=1}^{N} h_t (T_{crit,t} - T_{opt,t}) \begin{cases} h_t = 1\ h \text{ if } T_{op,t} \leq T_{crit,t} \\ h_t = 0 \quad \text{if } T_{op,t} > T_{crit,t} \end{cases} \tag{18B}$$

3.6 Comparison of ventilation modes

Looking at ventilation modes that were assessed in previous studies conducted by Geros et al. (1999), Givoni, (1998), and Kubota et al. (2009), it was decided that it was necessary to determine how the building would have performed had night ventilation not been utilized. To understand how each building would have performed without night ventilation, a simulation was run for each building with and without the presence of night ventilation, using the previously described temperature prediction model. For the purpose of this analysis, mechanical night ventilation in LEES occurs whenever the airflow rate goes above 700 CFM during unoccupied hours, and natural night ventilation occurs in IND and BH whenever the window is opened for any duration during unoccupied hours. For IND and BH, the non-night ventilation case is defined as days in which the window is closed for the entire day and night. For LEES, there are two forms of the non-night ventilation case. The first is termed regular airflow mode, in which the airflow is at its minimum code-required value and there is no daytime or nighttime cooling. The second is termed daytime cooling mode, in which the airflow is ramped up during occupied daytime hours. To assess performance in each ventilation mode, the performance metrics discussed in section 3.3 were calculated for the simulations with real inputs, and for simulations with no night ventilation, and later compared. A p-value $< .05$ was considered satisfactory for all t-tests conducted.

3.7 Optimization

Using the model generated for each building, an optimization was run to determine a control strategy that would minimize energy usage, limit changing window state, and maintain comfort. This optimization technique is a combination of those taken by Medved et al. (2014) and Zhang et al. (2014). LEES controls were optimized by minimizing airflow rate and temperature deviation from the ACS acceptability limits, rather than constraining the temperature, which allows for flexibility in the system. Because BH and IND do not consume energy with their night ventilation scheme, the BH and IND optimizations were conducted by minimizing only the temperature deviation from the ACS acceptability limits. This process was completed in Matlab. After the model was optimized, DDH was calculated with a temperature threshold of ACS upper 80% acceptability limit, and compared to the DDH of measured data.

4. Results

4.1 Baseline data analysis results

Figures 1-3 show selected conditions in the three buildings, examining one day in which night ventilation was successfully executed during the hottest week in each location. Table 4 summarizes the dates of the selected periods, how day vs. night airflow rates (or window status) changed, and comparisons of indoor and outdoor temperature metrics calculated from the raw data for that week (and visually represented in Figures 1-3). The delay in peak indoor temperature is equal to the amount of time between the occurrence of the peak outdoor and peak indoor air temperatures. The decrease in air and mass temperature during the night ventilation period is equal to the difference in each temperature occurring at the start time and end time of night ventilation. Table 5 summarizes the sample sizes and median values of performance metrics (defined at the beginning of Section 3.4, and in Eqns 10-16) that were calculated over the entire data set for each building.

Parameter	LEES	IND	BH
Start time of night ventilation (hr)	2	22	17
End time of night ventilation (hr)	8	7.5	7
Night ventilation condition	1100-1500 CFM	Windows open	Windows open
Diurnal swing (°F)	26	27	23.5
Peak outdoor temperature (°F)	86	82	102
Time of peak outdor temperature (hr)	13	14	14
Peak indoor temperature (°F)	76.5	74	88
Time of peak indoor temperature (°F)	15	20	19
Delay in peak indoor temperature (hr)	2	8	5
Decrease in air temperature during night ventilation period (°F)	6.5	5	3.5
Decrease in mass temperature during night ventilation period (°F)	3.5	0	3.5

Table 4. Data summary from hottest weeks

Parameter	LEES	IND	BH
Sample size (d)	842	60	357
Median $T_{I,max}$ (°F)	71	73.5	86
Median $Damp_{max}$ (°F)	2	7	9
Median TL (hr)	0	0	6
Median $T_{I,range}$ (°F)	3	2	3
Median f (%)	20	10	20

Table 5. Data summary from entire data set

As can be seen in Figures 1-3, for all the buildings the night ventilation strategy was successful in reducing the indoor air and mass temperatures, keeping the range of both fairly narrow, and consistently delaying the peak daily indoor temperatures. In LEES and BH, the mass floor temperature was similar to indoor air temperature during the day, and the air temperature dropped lower during the nighttime ventilation, as would be expected. In contrast, in IND, the air temperature was slightly higher than the mass during both the day and night, probably because the heaviness of the mass delayed its temperature rise by longer than a 24 hour period, thus allowing it to remain lower than air temperature for the entire duration of the day. For both LEES and BH, the patterns in the figures were typical of the rest of the hottest week, where indoor air temperature and mass temperature tracked each other very closely. There were exceptions during two nights in LEES when night ventilation airflow rates were extended for longer periods, resulting in indoor air dropping even lower than mass temperature. For IND, while instantaneous damping has such a large range of values, the strategy did not seem to impact the mass temperature or delay the peak indoor air temperatures. It is possible that the indoor air temperature and mass temperature have little fluctuation due to the fact that the mass is so heavy that it is effectively maintaining constant indoor temperatures without the need for additional passive cooling.

From Table 5, the low temperature peaks seen in the entire dataset for LEES would indicate that the strategy is successfully lowering the indoor temperature throughout the hot periods of the year. The median maximum damping values are fairly low, but this could be explained by the mild climate and fairly low outdoor temperatures. When comparing these parameters across classrooms, the maximum temperature seemed to be higher and maximum damping seemed to be lower in rooms on the southern side of the building. This is probably the case because these rooms have solar exposure for a greater amount of time and stronger intensity. Comparing across classrooms, the daily temperature range and daily decrement factor were noticeably larger for rooms on the second floor, especially those with south facing walls. This is probably due to the fact that they are not ground-coupled and the first story rooms have higher night ventilation airflow setpoints. Looking at the energy removed, as well as the potential energy efficiencies that are all above 1 (indicating that the strategy is removing more energy than is being consumed), confirms that the strategy is effective with respect to energy as well as comfort. Comparing across classrooms, the three rooms that were running with increased airflow rates for a larger portion of time removed significantly more energy, as would be expected.

Looking at the IND data in Table 5, the large range in maximum damping values and very narrow range of indoor temperature peaks suggests that damping is fairly independent of the indoor temperature and depends almost entirely on the outdoor temperature. This suggest that the time of indoor air temperature peak is independent of the outdoor temperature, and probably dominated by the internal load. It should be noted that the median range of indoor air temperature is very small, further suggesting that the indoor air temperature is not reliant on the outdoor air temperature in this building.

Moving now to BH in the unique seasons of India, the box-and-whisker plots in Figure 4 complement the data summarized in Table 5. Daily peak temperature is highest during the Pre-Monsoon and Monsoon seasons, probably because these have the highest outdoor temperatures. In contrast, daily maximum damping was lowest during the Pre-Monsoon and Monsoon seasons, indicating that even though the outdoor temperatures are higher, the indoor temperatures are maintaining consistent values. Time lag stayed fairly consistent across seasons. The daily energy removed is significantly higher for the Monsoon season than any other season, probably because this season has the strongest winds.

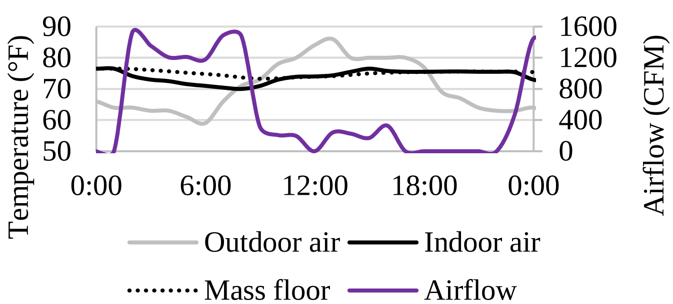

Figure 1. LEES room 233 temperature and airflow profile during and after night ventilation

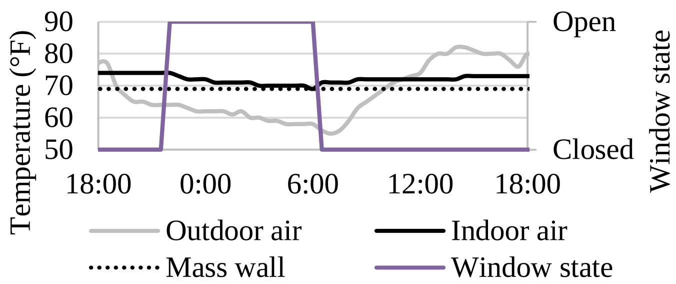

Figure 2. IND temperature and window state profile during and after night ventilation

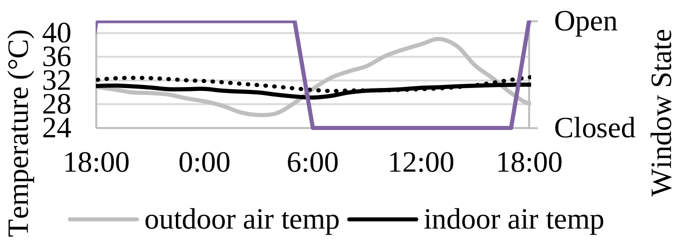

Figure 3. BH temperature and window state profile during and after night ventilation

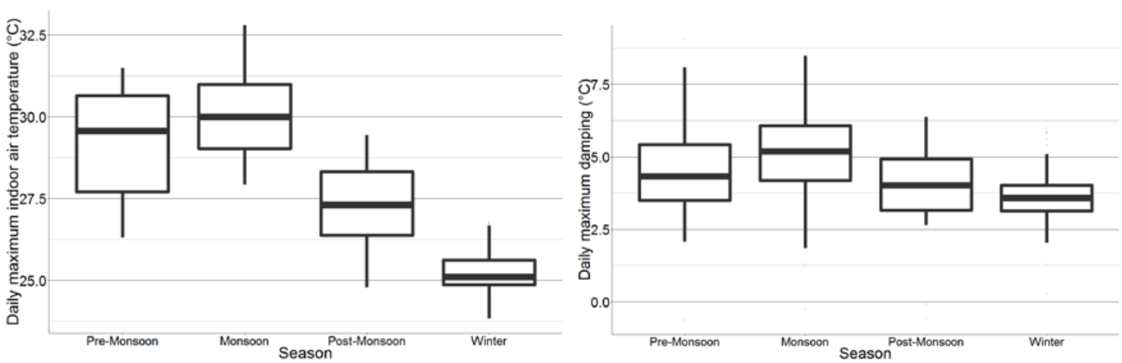

Figure 4. A) BH daily maximum indoor air temperature by season; B) BH daily maximum damping by season

4.2 Comparison to comfort standards results

The data was analyzed with respect to the existing comfort standards. As seen in Figure 5, during the 2-3 months of monitoring in each LEES classroom, the operative temperature never exceeded the upper ACS comfort limit, but tended to hover around the lower ACS comfort limit and in some instances even go below the limit, indicating that the space is being overcooled. With respect to the lower comfort limit, each classroom has at least a few days in which the daily DDH exceeds 0 (approximately 19% of data). The average daily DDH across all 8 classrooms is 0.46 °C-h (0.82 °F-h), and in some instances, the daily DDH reached as high as 13.3 °C-h (24 °F-h).

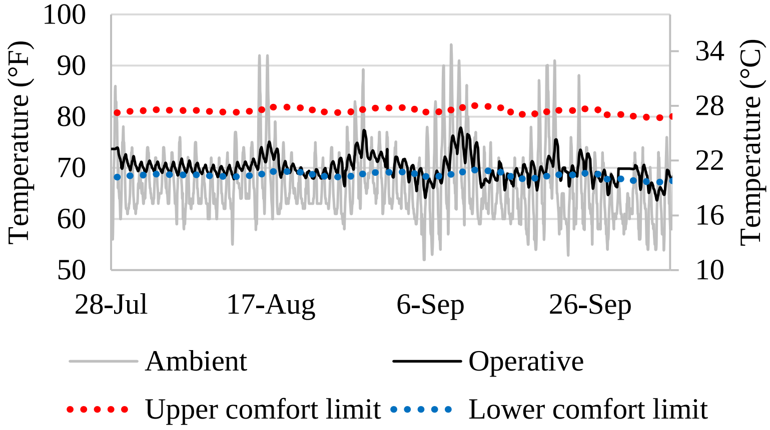

Figure 5. LEES room 233 operative temperature with ACS limits

As seen in Figure 6, during the two months of monitoring in IND, the operative temperature never exceeded the upper ACS comfort limit or dropped below the lower limit, and therefore the daily DDH never exceeds 0. That being said, the operative temperature seemed to stay very close to the lower ACS comfort limit, indicating that there is little need for additional cooling.

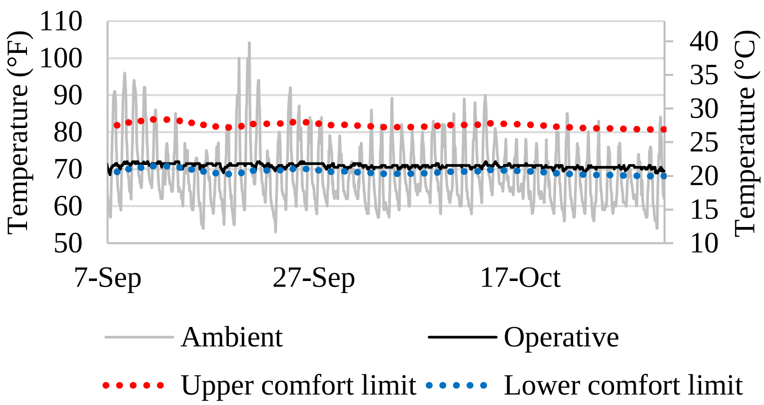

Figure 6. IND operative temperature with ACS limits

In analyzing the full year of data from BH with respect to IMAC, as shown in figure 7, the operative temperature never exceeded the upper IMAC comfort limit or fell below the lower IMAC limit. However, when comparing the data to the ACS comfort limits, it was found that the operative temperature exceeded the upper ACS comfort limit for approximately 12% of the year, during the Pre-Monsoon and Monsoon seasons. There is a wide spread of operative temperature across the year, but the operative temperature remains closer to the upper comfort limits for a higher proportion of the year. The average daily DDH across the year is approximately 0.38 °C-h. The daily DDH (with respect to the upper ACS comfort limit) exceeds 0 for 42% of the Pre-Monsoon season and 37% of the Monsoon season. During the Pre-Monsoon season, the average daily DDH is 0.58 °C-h and goes as high as 6 °C-h. During the Monsoon season, the average daily DDH is 0.68 °C-h and goes as high as 9.5 °C-h. The total DDH for the entire year is 131.7 °C-h.

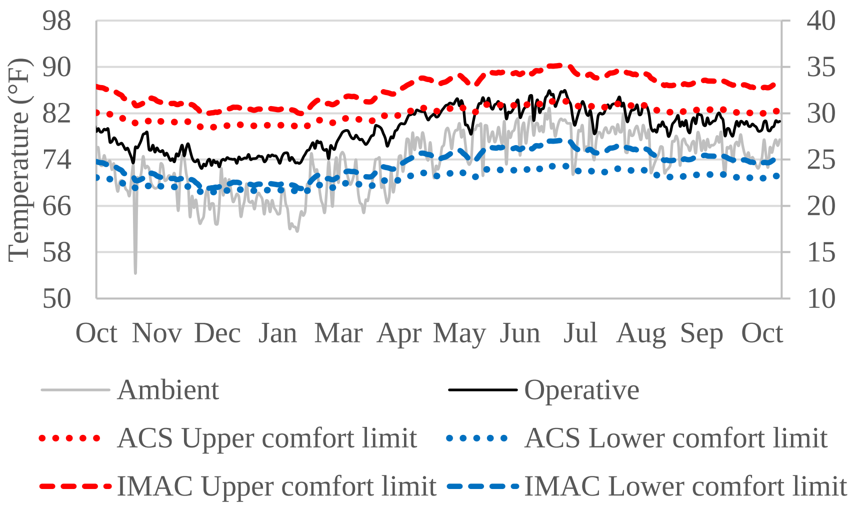

Figure 7. BH operative temperature with ACS & IMAC comfort limits

4.3 Temperature model selection

Temperature prediction models were generated for each of the case studies in order to simulate the buildings with and without night ventilation. The inputs and outputs of each model can be seen in table 6. Because each of the models was nonlinear in the inputs and states, they were linearized. The dynamical equations for the LEES, IND, and BH models, along with the model error parameters for each set of training data, can be found in Landsman (2016). The mean absolute error ranged from 0.2 °C (0.4 °F) to 0.7 °C (1.2 °F) error parameters for each set of training data are found in table 5. Figure 8 visualizes the real and simulated training data for LEES indoor air temperature.

Model parameters		**LEES**	**IND**	**BH**
Controllable inputs	Ventilation rate	X		
	Supply temp	X		
	Window state		X	X
Uncontrollable inputs	Outdoor air temp	X	X	X
	Solar radiation	X		X
	Internal loads		X	
Outputs	Indoor air temp	X	X	X
	Mass wall temp	X	X	X
	Mass floor temp	X	X	X

Table 6. Temperature model inputs and outputs

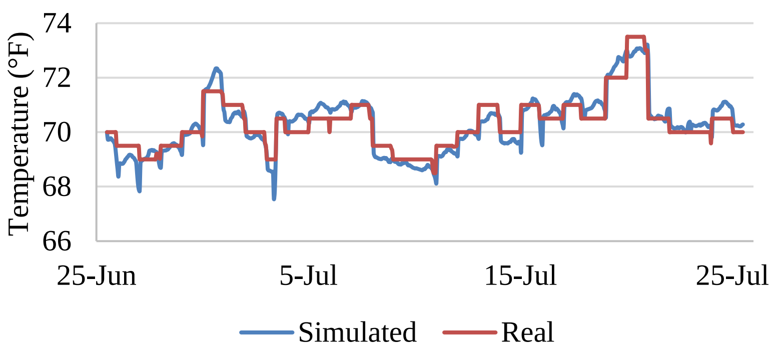

Figure 8. Real and simulated indoor air temperature in LEES room 110

4.4 Comparison of ventilation mode results

For LEES, no statistically significant differences were seen between model simulations with different ventilation inputs with regard to daily maximum indoor temperature, daily maximum damping, daily temperature range, decrement factor, or daily discomfort degree hours. This indicates that, in the context of these buildings and climates, the airflow rate has a very small influence on the indoor conditions, which are much more closely correlated to the supply temperature. In contrast, there *was* a statistically significant difference between models with regard to energy removed and potential energy efficiency, with different ventilation inputs. All of the models with simulated ventilation inputs removed less energy than those with real inputs. The simulated ventilation models are probably removing less heat because the real building is going into night ventilation or daytime cooling more often than the design control sequence calls for, which calls into question how the control sequence has changed since operation began. In addition, the simulated ventilation models may have lower potential energy efficiency because the real building is often not ventilating the building during occupied hours, whereas the simulated ventilation models are forced to have a code required minimum airflow rate during occupied hours, causing them to consume more fan energy.

For IND, no statistically significant differences were seen between model simulations with and without night ventilation with regard to daily maximum indoor temperature, daily maximum damping, or daily discomfort degree hours. This indicates that the strategy was not having a large impact on the internal conditions. The only metrics that showed statistically significant differences with and without night ventilation were daily temperature range and decrement factor, both of which were higher for the case with night ventilation. This is probably the case because the night ventilation allowed for a slight temperature reduction at night, thus increasing the daily temperature range.

For BH, performance metrics were compared using model simulations with night ventilation (NV) and without night ventilation (no NV), with a total sample size of 712 d (356 with NV and 356 without NV). Statistically significant differences were seen between model runs with and without night ventilation with regard to daily maximum indoor air temperature and daily maximum damping. However, on average, maximum indoor temperature and maximum damping were less than 1 °C different for model runs with and without night ventilation, even during the warmest seasons of the year (figures 9A and 9B). Although the indoor temperature peaks are only lower by 0.6-0.7 °C and the maximum damping is only higher by 0.6-0.7 °C for the night ventilation simulation, this is still improving the indoor conditions and can help improve comfort when paired with other strategies. No statistically significant differences were seen between model runs with and without night ventilation with regard to time lag, which matches the results from section 5.3.3.

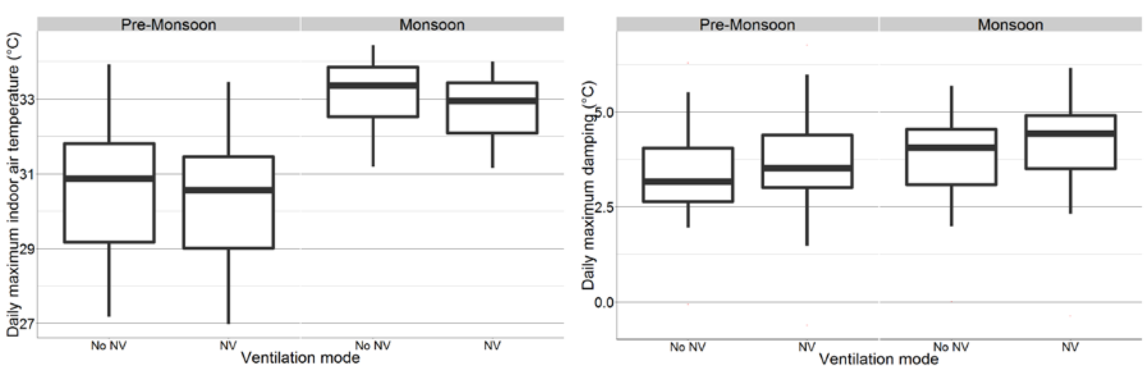

Figure 9. A) BH simulation daily maximum indoor air temperature; B) BH simulation daily maximum damping

Finally, statistically significant differences were seen between model runs with and without night ventilation with regard to daily discomfort degree hours above the maximum comfort limit. On average, the model run with night ventilation had 3.5 °C-h less than the model run without night ventilation in the Pre-Monsoon and Monsoon seasons (figure 10). This difference could have a large impact on the comfort of the occupants inside the space.

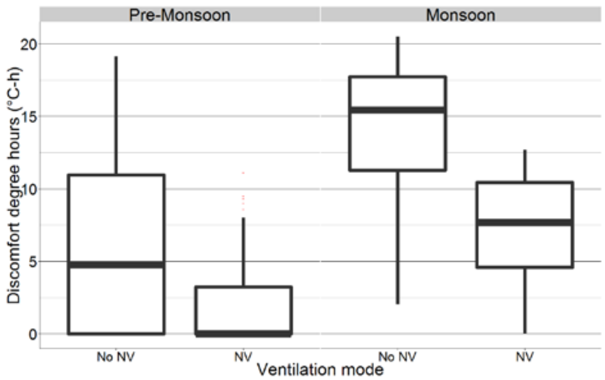

Figure 10. BH simulation daily discomfort degree hours above maximum ACS limit with & without night ventilation

4.5 Optimization

The controls for each building were optimized to minimize energy and maximize comfort (by minimizing the time outside the comfort limits). After running the optimization for LEES, the system operated with only minimum allowable airflow. This suggests that these classrooms need no night ventilation to satisfy comfort requirements.

The window state of IND was optimized for one week in September in which the outdoor temperature went above 100 °F. This resulted in keeping the windows open for a longer duration than the actual building controls suggested. A comparison was done between the models with optimized window state and real window state with a total sample size of 14 d (7 d with real inputs and 7 d with optimized inputs). The optimized model consistently kept the operative temperature at an equivalent or lower level (by approximately 1 °F) than the model with real inputs.

The window state of the BH was optimized for one week in April in which the operative temperature went above the upper ACS comfort limit (see figure 11). Surprisingly, the optimization resulted in keeping the windows closed for more nights than the occupants did themselves. A comparison was done between the models with optimized window state and real window state with a total sample size of 14 d (7 d with real inputs and 7 d with optimized inputs). The optimized model consistently kept the operative temperature at an equivalent or lower level (by approximately 5 °F) than the model with real inputs. The optimized model was also able to bring the operative temperature below the upper comfort limit on certain days that originally fell above the limit.

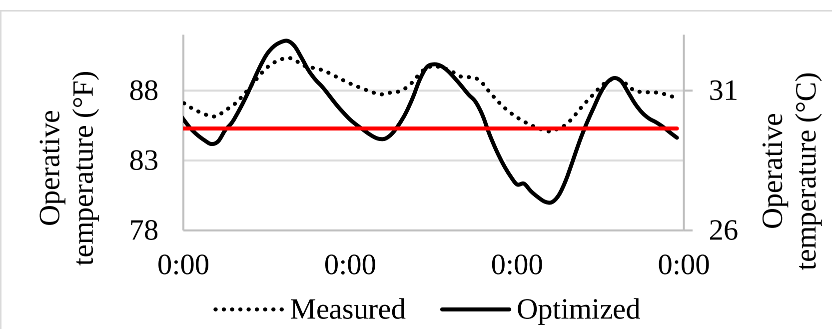

Figure 11. BH measured, optimized, & no NV operative temperature

4.6 Occupant behavior model selection

An occupant behavior prediction model was generated for the Blessing House to understand how the occupants were controlling the night ventilation scheme. The selected model uses inputs of season, hour, outdoor air temperature, indoor air temperature, and mass temperature. The regression constants, seen in Table 7, indicate that the most influential variables on window opening behavior are indoor air temperature and mass temperature. The model achieved 81.2% accuracy for the training data and 86.6% accuracy for the validation data. Figure 12 visualizes the window opening probably by each variable for the Pre-Monsoon season.

Variable	Regression Constant
Intercept	-4.78
Season (Pre-Monsoon)	1.00
Season (Monsoon)	0.089
Season (Post-Monsoon)	0.14
Season (Winter)	-1.45
Hour	-0.057
Outdoor air temperature	-0.22
Indoor air temperature	-1.18
Mass temperature	1.56

Table 7. Occupant behavior model regression constants

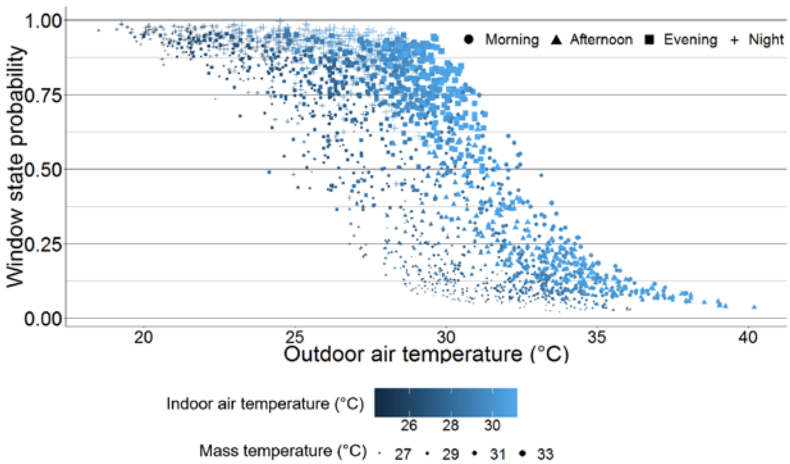

Figure 12. Window opening probability for Pre-Monsoon season

5. Discussion

The results of this study clearly suggest that the night ventilation strategy, in combination with the physical construction of the building, is successfully keeping LEES below the maximum comfort limit during hot periods. This said, results of the predictive modeling suggests that the airflow rate has very little impact on the indoor conditions. This goes against the findings of Kolokotroni and Aronis, (1999), who saw that higher airflow rates lead to increased energy savings. One possible explanation for this disagreement between model results and measured results is the fact that the airflow rate might have more impact on the indoor conditions during warmer days, and the data used for parameter identification might not have included the hottest days of the data set. Regardless of the impact of airflow rate, the indoor temperature is still significantly dampened compared to the outdoor air temperature.

Although the space is being successfully cooled, the strategy is sometimes overcooling the classrooms, which suggests that there may be a mismatch between the design intent and patterns of operation in the building, and the system may actually be using more energy in the morning to warm up the space before occupancy. There are a few explanations for this overcooling, one being that the mass temperature setpoint for entering night ventilation is simply too low. This corresponds with the findings of Kolokotroni and Aronis (1999), which saw increased energy consumption at lower temperature setpoints. Another is that the specification of a difference of 5.6 °C (10 °F) between mass temperature and outdoor air temperature for entering night ventilation is too high, especially because this occurs so often in the mild climate. It is very telling that when the controls were optimized to minimize time outside of the comfort bounds, the system never entered night ventilation mode. It is recommended that the building operator increase the mass temperature setpoint or reduce the necessary difference between outdoor and mass temperature for entering night ventilation.

Although the system consistently had very high energy efficiency, the fact that the space was being overcooled suggests that there is still energy being wasted by running the fans too often. As seen in the measured data, some of the classrooms achieved similar indoor temperatures both with and without night ventilation, probably due to the very mild climate. This matches the findings of Kolokotroni and Aronis (1999a), who observed increased energy usage during mechanical night ventilation in a medium weight office building, due to the increased operation of fans. If the increased airflow is not necessary to achieve the same condition, this fan energy could be saved and a similar amount of heat could still be dissipated through the mass. In addition, the energy consumed to reheat the space in the morning was not taken into consideration in this calculation, as the energy efficiency was only examined for heat removed.

While the study suggests that the strategy is overcooling, the applicability of the adaptive comfort model to schools is still in question. The LEES ventilation system is not controlled by its occupants, so its not clear how much the adaptive effect might exist; additionally, the adaptive comfort model has not been thoroughly tested in schools with young children. One study that took place in a naturally ventilated elementary school found that the observed lower 80% acceptability limit was 1.7 °C below the value listed in the ASHRAE standard (Hwang et al. 2009). Another study that took place in a naturally ventilated elementary school saw that the predicted thermal acceptability according to the adaptive comfort model did not match the surveyed acceptability values (Kwok and Chun 2003).

Turning now to IND, the results of this study suggest that its night ventilation strategy, in combination with the physical construction of the building, has no discernable impact on the internal conditions of the space. The most likely reason for the low impact of night ventilation is the extremely high level of thermal mass and low internal loads. This matches the findings of Kolokotroni et al. (1999a), Geros et al. (1999), and Pfafferott et al. (2004), who saw that night ventilation efficiency increased during periods with lower internal gains and that user behavior and internal loads have a stronger effect on internal temperature in milder climates. However, this goes against the findings of Finn et al. (2007), Givoni (1998), Shaviv et al. (2001), and Kolokotroni and Aronis (1999), whose studies all indicated that higher levels of thermal mass improve the performance of night ventilation. The very thick concrete walls and floor are likely able to take care of the load all on their own, providing sufficient thermal mass to reduce the range of indoor temperature, which in turn prevents a noticeable additional effect from night ventilation. Another explanation is that because the ratio of wall to floor area is fairly small, the size of the thermal mass has a less significant impact on the performance, which would match the results of Artmann et al. (2008). It is entirely possible that the night ventilation strategy would have a larger impact if the mass was less heavy or if the internal loads were higher. Like LEES, the applicability of the adaptive comfort model to IND is also in question because of the lack of occupant control.

The results of this study suggest that the night ventilation strategy in BH, in combination with the physical construction of the building, successfully lowers the indoor temperature, removes heat from the space, and reduces discomfort degree hours, especially during the hottest seasons of the year. This is very significant because the strategy implemented in BH is very simple and the night ventilation is not always believed to work successfully in hot and humid climates, as shown by Da Graça et al. (2002) and Liping and Hien (2007), who found that night ventilation did not help improve the indoor conditions in Shanghai and Singapore compared to daytime ventilation. However, the results from BH seem to correspond with the findings of Kubota et al. (2009), who saw saw a reduction of maximum indoor air temperature when nighttime ventilation was implemented in a study in the hot and humid climare of Malaysia.

Although the strategy is successful, the effect size of damping the indoor temperature due to night ventilation is fairly small. Although small differences in temperature can make a larger difference in climates with high humidity, the strategy probably cannot achieve enough on its own to take care of the entire load. Night ventilation, paired with other low energy strategies such as ceiling fans, has the potential to maintain comfort in this climate. In analyzing comfort with measured data, the annual discomfort degree hours was approximately 131.7 °C-h. If the air speed were increased to 0.6 m/s through the use of ceiling fans, the annual discomfort degree hours drops to 2.6 °C-h, and 0 °C-h at air speeds above 0.6 m/s. This was calculated using the adjusted adapative comfort model limits for increased air speeds.

The results of the window opening behavior model suggest that occupants' decision to open or close windows is most closely correlated to the indoor air temperature and mass temperature. This matches the result of the behavior model developed by Yun and Steemers (2008), which also had a close relationship with indoor temperature and poor correlation to outdoor temperature. It is somewhat of a surprise that the outdoor air temperature was not very influential on the behavior model for BH, as the occupants indicated that they thought outdoor air temperature was a trigger for window control. The impact of mass temperature is also significant because this is not a parameter that the occupants consciously took into consideration, which indicates that the inclination to open or close the windows could be subconscious and more related to the occupants' thermal sensation. It should also be noted that although the model was developed specifically for occupants in this building, the methodology can be applied to other buildings.

Although no generalizable conclusions can be drawn about the effect of each night ventilation parameter based on just three case studies, each in such different climates with such different controls, a number of extrapolations can be made. First looking at daily maximum indoor air temperature, BH had a much higher average than the other two buildings, but this can simply be attributed to the fact that BH is in a much hotter climate. On the other hand, there was only a 0.56 °C (1 °F) difference between LEES and IND average values, which suggests that different levels of mass and types of night ventilation were resulting in approximately the same daily temperature peaks. With regard to daily maximum damping, BH and IND had a much higher effect size than LEES. The only obvious similarity between BH and IND is the use of natural night ventilation. It is possible that natural night ventilations lends itself to higher values of maximum damping due to the fact that the open windows allow the space to more closely follow nighttime temperatures, whereas air must travel through ducts for mechanical night ventilation, possibly gaining some heat along the way.

With regard to daily time lag and temperature range, BH had a much higher effect size than LEES and IND. These two metrics are probably closely related. Due to the fact that the mild climates in LEES and IND kept their temperature range so low, the indoor air temperature did not require much time to peak. In BH, the temperature range was wider and thus required more time to hit that peak.

In conclusion, the fact that both LEES and IND had indoor conditions near the bottom or below the ACS lower comfort limit indicates that night ventilation could have the tendency to overcool when used in mild climates, and that cooling by night ventilation may not even be needed once you have sufficient mass. In addition, the similar performance in IND and LEES shows that the type of ventilation system and control sequence are probably less significant to the performance of the strategy than the climate it is used in. Finally, the overall performance of night ventilation seemed to be better in BH than LEES or IND, possibly suggesting that the strategy might be better suited to hotter climate.

6. Limitations

There are numerous limitations to this study, most of which are attributed to the limited availability of data. Firstly, many parameters critical to the model calculations conducted in this study were not available and therefore had to be estimated. Another major limitation to the study is the simplicity of the model generated for comparison. Although this model achieved very small errors compared to measured data, the model still utilizes very simplified dynamical equations, and therefore cannot truly capture the dynamics of the heat in the space. The final limitation to this study is the lack of a control case. In terms of the performance within each individual buildings, there was no control period in which night ventilation was not used.

7. Conclusions

Measured data of indoor environmental conditions were obtained from three different buildings, each using night ventilation for cooling, with varying control strategies (both mechanical and natural), climates (mild and hot/humid), and levels of thermal mass (medium and heavy). The design and configuration of each building's control strategy was then investigated and laid out in detail.

Subsequently, the performance of night ventilation in each building with regard to indoor thermal conditions was assessed using measured data and comparing it to an adaptive comfort model. The results indicated that the buildings using the night ventilation strategy in a mild climate are successfully keeping the indoor operative temperature below the upper 80% acceptability comfort limit. However, the case studies in the mild climate are also cooling more than necessary at times, sometimes bringing the operative temperature at or below the lower 80% comfort limit. The building in the hot and humid climate is going above the upper 80% comfort limit on the hottest days of the year, but still keeping the operative temperature within the comfort bounds for 88% of the year.

Next, a hybrid model was developed for each case study, based on simplified resistance/capacitance equations, to predict the indoor conditions of the building with inputs including outdoor air temperature, solar radiation, internal loads, ventilation rate, and window state. These models were then fit to a training data set and validated against measured data, each providing temperature predicitions with acceptable error.

For the building with medium mass and using mechanical night ventilation in a mild climate, there were no significant differences in internal conditions between the different ventilation modes. For the buiding with heavy mass and using automated natural night ventilation in a mild climate, the indoor temperature had very little fluctuation and there were no significant differences between cases with and without night ventilation, most likely due to the impact of the heavy mass and mild climate. For the building with medium mass and using manual natural night ventilation in a hot and humid climate, the night ventilation strategy successfully lowered indoor temperatures and helped remove heat, but could not remove enough on its own to satisfy comfort requirements.

Using the predictive model, the control strategy for each building was optimized to minimize the amount of time outside of the comfort bounds. In the two buildings in the mild climate, because the night ventilation strategy had such a small impact on the internal conditions of the buildings, the optimized controls did not demand any night ventilation. On the other hand, the building in the hot and humid climate saw an even further reduction in discomfort degree hours after the controls were optimized.

Finally, a statistical model was successfully developed to predict the window opening pattern for occupants of the Blessing House. It was discovered that the parameters that have the strongest impact on opening or closing the windows are indoor air temperature and mass temperature.

Acknowledgements

We would like to thank the Center for the Built Environment and the Center for Building Energy Research and Development for providing funding and provision for this project. Additionally, this study was made possible thanks to all of the individuals who helped bring these case studies to our attention and collect data for these buildings. This includes Glenn Friedman and Brent Eubanks for the La Escuelita Elementary School, Neil Burger, Shannon Allison, and Eric Sande for 435 Indio Way, and Vijai Krishnaraj for the Blessing House.

References

Artmann, N., H. Manz, and P. Heiselberg. 2008. “Parameter Study on Performance of Building Cooling by Night-Time Ventilation.” *Renewable Energy* 33 (12): 2589–98. doi:10.1016/j.renene.2008.02.025.

Blondeau, Patrice, Maurice Spérandio, and Francis Allard. 1997. “Night Ventilation for Building Cooling in Summer.” *Solar Energy* 61 (5): 327–35.

Borgeson, Sam, and Gail Brager. 2008. “Occupant Control of Windows: Accounting for Human Behavior in Building Simulation.” *eScholarship*, October. http://escholarship.org/uc/item/5gx2n1zz.

Da Graça, G. Carrilho, Q. Chen, L. R. Glicksman, and L. K. Norford. 2002. “Simulation of Wind-Driven Ventilative Cooling Systems for an Apartment Building in Beijing and Shanghai.” *Energy and Buildings* 34 (1): 1–11.

Dear, Richard J. de, and Gail Schiller Brager. 1998. “Developing an Adaptive Model of Thermal Comfort and preference/Discussion.” *ASHRAE Transactions* 104: 145.

Fanger, Poul O., and others. 1970. “Thermal Comfort. Analysis and Applications in Environmental Engineering.” *Thermal Comfort. Analysis and Applications in Environmental Engineering.* http://www.cabdirect.org/abstracts/19722700268.html.

Finn, Donal P., Darragh Connolly, and Paul Kenny. 2007. “Sensitivity Analysis of a Maritime Located Night Ventilated Library Building.” *Solar Energy* 81 (6): 697–710. doi:10.1016/j.solener.2006.10.008.

Gagge, A. Pharo, A. P. Fobelets, and LoG Berglund. 1986. “A Standard Predictive Index of Human Response to the Thermal Environment.” *ASHRAE Trans.;(United States)* 92 (CONF-8606125-). http://www.osti.gov/scitech/biblio/6494216.

Gagliano, A., F. Patania, F. Nocera, and C. Signorello. 2014. “Assessment of the Dynamic Thermal Performance of Massive Buildings.” *Energy and Buildings* 72 (April): 361–70. doi:10.1016/j.enbuild.2013.12.060.

García, Carlos E., David M. Prett, and Manfred Morari. 1989. “Model Predictive Control: Theory and practice—A Survey.” *Automatica* 25 (3): 335–48. doi:10.1016/0005-1098(89)90002-2.

Geros, V., M. Santamouris, A. Tsangrasoulis, and G. Guarracino. 1999. “Experimental Evaluation of Night Ventilation Phenomena.” *Energy and Buildings* 29 (2): 141–54.

Givoni, Baruch. 1992. “Comfort, Climate Analysis and Building Design Guidelines.” *Energy and Buildings* 18 (1): 11–23.

———. 1998. “Effectiveness of Mass and Night Ventilation in Lowering the Indoor Daytime Temperatures. Part I: 1993 Experimental Periods.” *Energy and Buildings* 28 (1): 25–32.

Hwang, Ruey-Lung, Tzu-Ping Lin, Chen-Peng Chen, and Nai-Jung Kuo. 2009. “Investigating the Adaptive Model of Thermal Comfort for Naturally Ventilated School Buildings in Taiwan.” *International Journal of Biometeorology* 53 (2): 189–200. doi:10.1007/s00484-008-0203-2.

Kolokotroni, M., and Aj Aronis. 1999a. “Cooling-Energy Reduction in Air-Conditioned Offices by Using Night Ventilation.” *Applied Energy* 63 (4): 241–53.

———. 1999b. “Cooling-Energy Reduction in Air-Conditioned Offices by Using Night Ventilation.” *Applied Energy* 63 (4): 241–53.

Kolokotroni, M., B. C. Webb, and S. D. Hayes. 1998. “Summer Cooling with Night Ventilation for Office Buildings in Moderate Climates.” *Energy and Buildings* 27 (3): 231–37.

Kubota, Tetsu, Doris Toe Hooi Chyee, and Supian Ahmad. 2009. “The Effects of Night Ventilation Technique on Indoor Thermal Environment for Residential Buildings in Hot-Humid Climate of Malaysia.” *Energy and Buildings* 41 (8): 829–39. doi:10.1016/j.enbuild.2009.03.008.

Kwok, Alison G, and Chungyoon Chun. 2003. “Thermal Comfort in Japanese Schools.” *Solar Energy* 74 (3): 245–52. doi:10.1016/S0038-092X(03)00147-6.

Liping, Wang, and Wong Nyuk Hien. 2007. “The Impacts of Ventilation Strategies and Facade on Indoor Thermal Environment for Naturally Ventilated Residential Buildings in Singapore.” *Building and Environment* 42 (12): 4006–15.

Manu, Sanyogita, Yash Shukla, Rajan Rawal, Leena E. Thomas, and Richard de Dear. 2016. “Field Studies of Thermal Comfort across Multiple Climate Zones for the Subcontinent: India Model for Adaptive Comfort (IMAC).” *Building and Environment* 98 (March): 55–70. doi:10.1016/j.buildenv.2015.12.019.

Medved, Sašo, Miha Babnik, Boris Vidrih, and Ciril Arkar. 2014. “Parametric Study on the Advantages of Weather-Predicted Control Algorithm of Free Cooling Ventilation System.” *Energy* 73 (August): 80–87. doi:10.1016/j.energy.2014.05.080.

Moura, Scott J., Miroslav Krstic, and Nalin A. Chaturvedi. 2012. “Adaptive PDE Observer for Battery SOC/SOH Estimation.” In *ASME 2012 5th Annual Dynamic Systems and Control Conference Joint with the JSME 2012 11th Motion and Vibration Conference*, 101–110. American Society of Mechanical Engineers. http://proceedings.asmedigitalcollection.asme.org/proceeding.aspx?articleid=1739097.

Pfafferott, Jens, Sebastian Herkel, and Matthias Wambsganß. 2004. “Design, Monitoring and Evaluation of a Low Energy Office Building with Passive Cooling by Night Ventilation.” *Energy and Buildings* 36 (5): 455–65. doi:10.1016/j.enbuild.2004.01.041.

Santamouris, Matheos, and Demosthenes Asimakopoulos. 1996. *Passive Cooling of Buildings*. Earthscan. https://books.google.com/books?hl=en&lr=&id=tLHsJ0-vEkYC&oi=fnd&pg=PR9&dq=Passive+Cooling+of+Buildings&ots=MX1G-stuHi&sig=V03LDkXeMj3KLGzHfJa-bbw-aLs.

Santamouris, M., A. Sfakianaki, and K. Pavlou. 2010. “On the Efficiency of Night Ventilation Techniques Applied to Residential Buildings.” *Energy and Buildings* 42 (8): 1309–13. doi:10.1016/j.enbuild.2010.02.024.

Shaviv, Edna, Abraham Yezioro, and Isaac G. Capeluto. 2001. “Thermal Mass and Night Ventilation as Passive Cooling Design Strategy.” *Renewable Energy* 24 (3): 445–52.

Tsanas, Athanasios, and Angeliki Xifara. 2012. “Accurate Quantitative Estimation of Energy Performance of Residential Buildings Using Statistical Machine Learning Tools.” *Energy and Buildings* 49: 560–567.

Vidrih, Boris, Ciril Arkar, and Sašo Medved. 2016. “Generalized Model-Based Predictive Weather Control for the Control of Free Cooling by Enhanced Night-Time Ventilation.” *Applied Energy* 168: 482–92.

Yun, Geun Young, and Koen Steemers. 2008. “Time-Dependent Occupant Behaviour Models of Window Control in Summer.” *Building and Environment* 43 (9): 1471–82. doi:10.1016/j.buildenv.2007.08.001.

———. 2010. “Night-Time Naturally Ventilated Offices: Statistical Simulations of Window-Use Patterns from Field Monitoring.” *Solar Energy* 84 (7): 1216–31.

Zhang, Rongpeng, Yisu Nie, Khee Poh Lam, and Lorenz T. Biegler. 2014. “Dynamic Optimization Based Integrated Operation Strategy Design for Passive Cooling Ventilation and Active Building Air Conditioning.” *Energy and Buildings* 85 (December): 126–35. doi:10.1016/j.enbuild.2014.09.032.